

Intermolecular disulfide bonds between nucleoporins regulate karyopherin-dependent nuclear transport

Shige H. Yoshimura^{1,*}, Shotaro Otsuka¹, Masahiro Kumeta¹, Mariko Taga^{1,2,3} and Kunio Takeyasu¹

¹Graduate School of Biostudies, Kyoto University, Yoshida-konoe-cho, Sakyo-ku, Kyoto 606-8501, Japan

²Centre Mémoire de Ressources et de Recherche (CMRR) and Department of Histology and Biology of Aging, Groupe Hospitalier Lariboisière Fernand Widal Saint-Louis, APHP, Université Paris VII, Paris 75010, France

³INSERM U839 Institut du Fer à Moulin, Paris 75005, France

*Author for correspondence (yoshimura@lif.kyoto-u.ac.jp)

Accepted 14 April 2013

Journal of Cell Science 126, 3141–3150

© 2013. Published by The Company of Biologists Ltd

doi: 10.1242/jcs.124172

Summary

Disulfide (S–S) bonds play important roles in the regulation of protein function and cellular stress responses. In this study, we demonstrate that distinct sets of nucleoporins (Nups), components of the nuclear pore complex (NPC), form S–S bonds and regulate nuclear transport through the NPC. Kinetic analysis of importin β demonstrated that the permeability of the NPC was increased by dithiothreitol treatment and reduced by oxidative stress. The permeability of small proteins such as GFP was not affected by either oxidative stress or a reducing reagent. Immunoblot analysis revealed that the oxidative stress significantly induced S–S bond formation in Nups 358, 155, 153 and 62 but not 88 and 160. The direct involvement of cysteine residues in the formation of S–S bonds was confirmed by mutating conserved cysteine residues in Nup62, which abolished the formation of S–S bonds and enhanced the permeability of the NPC. Knocking down Nup62 reduced the stress-inducible S–S bonds of Nup155, suggesting that Nup62 and Nup155 are covalently coupled via S–S bonds. From these results, we propose that the inner channel of the NPC is somehow insulated from the cytoplasm and is more sensitive than the cytoplasm to the intracellular redox state.

Key words: Disulfide bridge, Importin β , Nuclear pore, Nucleocytoplasmic transport, Oxidative stress

Introduction

Disulfide (S–S) bond formation within and between proteins plays an important role in protein folding, stability, function, and protein–protein interaction. Reactive oxygen species (ROS) directly or indirectly oxidize the thiol group in cysteine residues, and thereby alter enzymatic functions (Kobayashi et al., 2006; Motohashi and Yamamoto, 2004; Pekovic et al., 2011; Rhee et al., 2005; Spickett et al., 2006; Winterbourn, 2008). The cytoplasm is normally maintained in a reducing state due to ubiquitous reducing reagents such as glutathione. However, ROS have been known to oxidize proteins in the cytoplasm. In the case of protein tyrosine phosphatase, one of the cysteine residues in the reactive center is oxidized by hydrogen peroxide (H_2O_2) and forms an intramolecular S–S bond, which results in the inhibition of phosphatase activity (Rhee et al., 2005). The transcription factor Nrf2 is also regulated by oxidative stress. Under non-stressed conditions, Nrf2 is ubiquitinated in a Keap1-dependent manner and subject to proteasome-dependent degradation. Under oxidative stress, however, specific cysteine residues in Keap1 are modified (Kobayashi et al., 2006). The modifications are thought to block Keap1 from binding to Nrf2, and thus increase the intracellular level of Nrf2, which results in the transcriptional activation of a series of genes related to oxidative responses (Motohashi and Yamamoto, 2004).

Macromolecular transport between the cytoplasm and the nucleoplasm is mediated by a large protein complex, the nuclear pore complex (NPC), which is composed of ~30 different kinds

of subunits called nucleoporins (Nups) (Brohawn et al., 2009). The NPC is a selective barrier that blocks the diffusion of large proteins (>40 kDa), but allows that of small proteins (<40 kDa) (Görllich and Kutay, 1999). The transport of large proteins is achieved by a number of transport mediators (karyopherins, also called importin β -family proteins) and the RanGDP–RanGTP gradient across the nuclear envelope (Mosammaparast and Pemberton, 2004; Weis, 2003). The importin α/β pathway is the best known route for transporting nuclear localization signal (NLS)-containing proteins from the cytoplasm to the nucleoplasm (Mattaj and Englmeier, 1998). It has been reported that oxidative stress inhibits macromolecular transport through the NPC (Crampton et al., 2009; Kodiha et al., 2004; Kodiha et al., 2009; Kodiha et al., 2008; Miyamoto et al., 2004; Patel et al., 2012; Stochaj et al., 2000; Yasuda et al., 2006). Oxidative stress influences the intracellular distribution of Ran and transport mediators, which in turn affects the intracellular localization of the cargo proteins (Kodiha et al., 2004; Kodiha et al., 2008; Yasuda et al., 2006). Oxidative stress also alters the modifications of Nups (phosphorylation and glycosylation), which might affect the passage of proteins through the NPC (Crampton et al., 2009; Kodiha et al., 2009).

In this study, we investigated the possibility of cysteine modifications of Nups, and their involvement in the regulation of nuclear transport. We found that several Nups form intermolecular S–S bonds, and that oxidative stress enhances such S–S bond formation and directly affects the transport of importin β through the NPC.

Results

Oxidative stress and reducing reagents alter importin β -dependent cargo transport

We first examined how oxidizing and reducing reagents affect protein transport through the NPC. HeLa cells were treated with digitonin at 4°C to remove the plasma membrane and the cytosolic proteins. The exposed nuclei were further incubated at 37°C to remove small soluble proteins from the nuclei. Immunofluorescence microscopic observation revealed that this treatment removed most of the intracellular Ran; no signal was seen in the cytoplasm and only weak signal was detected in the nucleoplasm (5% of the intact cells) (Fig. 1A). Immunoblot analysis also showed that 96% of Ran was removed by this treatment (Fig. 1B).

A mixture of recombinant transport mediators (importin α and β), fluorescently labeled cargo protein (glutathione S-transferase (GST)-NLS-GFP), and RanGDP was incubated with these nuclei in the presence of an ATP-regeneration system. Microscopic observation revealed that the fluorescent cargo was imported into

the nucleus from the external medium (Fig. 1C). When the same type of experiment was performed with the cells pre-exposed to oxidative stress (H_2O_2) for 1 hour, the nuclear cargo level decreased up to 0.43-fold as the H_2O_2 concentration increased (Fig. 1C,D), indicating that the permeability of the NPC is somehow affected by oxidative stress. On the other hand, pre-treatment of nuclei with dithiothreitol (DTT) increased the nuclear cargo level of both non-stressed and stressed cells by ~1.3-fold (Fig. 1E).

The intracellular ROS was quantified by a ROS-reactive fluorescence probe (carboxy- H_2DCFDA). As shown in Fig. 1F,G, the intracellular amount of ROS increased by oxidative stress. The pre-treatment of the cells by a ROS scavenger, *N*-acetyl cysteine (NAC, 10 mM), could reduce the ROS generation (Fig. 1G), and restore the stress-induced inhibition of nuclear import of NLS cargo (Fig. 1D). These results demonstrate that the stress-induced inhibition of nuclear transport results from the increase of the intracellular ROS level.

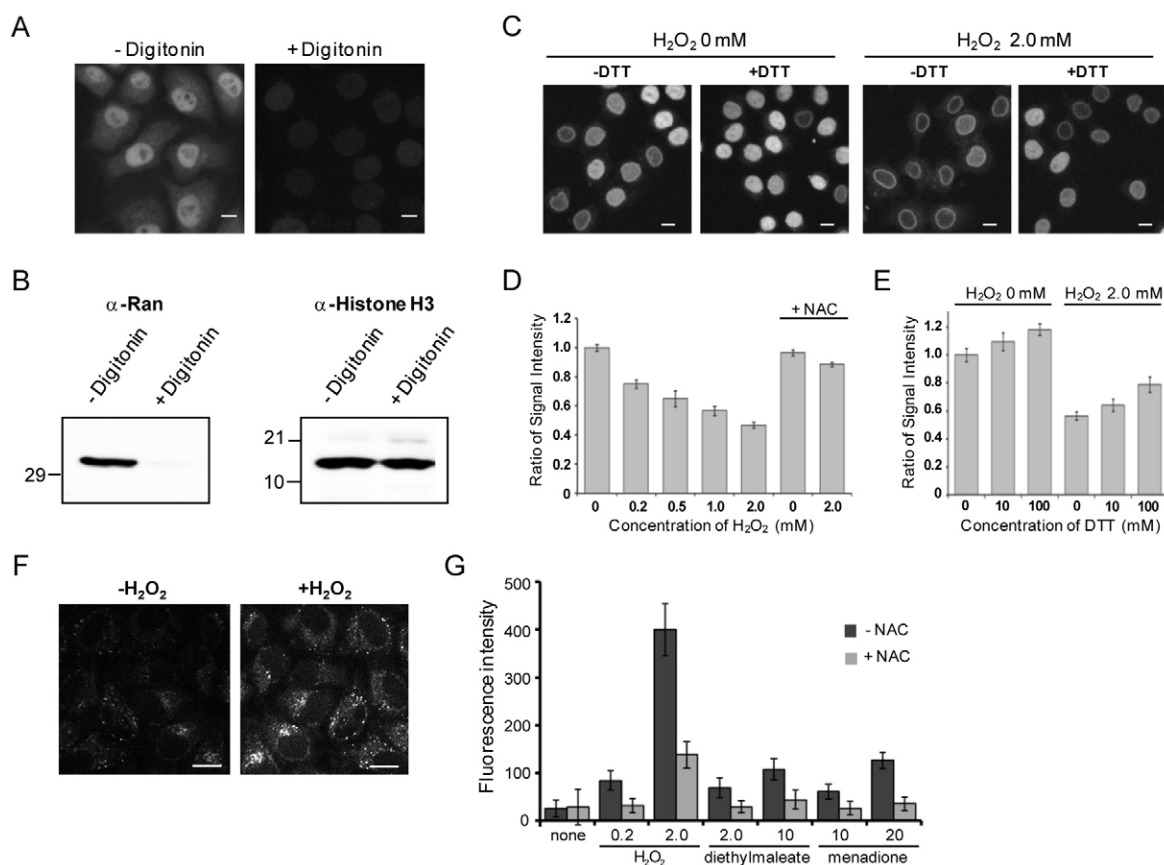


Fig. 1. Oxidative stress inhibits nuclear transport in permeabilized cells. (A,B) Digitonin treatment removes almost all endogenous Ran from the nucleus. (A) Digitonin-treated or non-treated HeLa cells were immunostained with anti-Ran antibody. (B) The digitonin-treated or non-treated HeLa cells were collected and subjected to SDS-PAGE and western blotting. Ran was detected using anti-Ran antibody. Histone H3 was also detected using anti-histone H3 antibody as a loading control. (C–E) HeLa cells were exposed to H_2O_2 for 1 hour. After washing, cells were permeabilized with digitonin, incubated with purified GST-NLS-GFP, importin α , importin β , Ran and ATP-regenerating system and observed by fluorescence microscopy (C). The signal intensity in the nucleus was quantified and represented in terms of its ratio to the signal from non-stressed cells (D). The same analysis was performed with permeabilized cells pre-treated with DTT before the addition of the import mixture (E). Error bars represent the s.e.m. of measurements from ~40 cells. (F,G) Oxidative stress increased the intracellular ROS level. A ROS-reactive fluorescence probe (carboxy- H_2DCFDA) was loaded to the cells before exposure to oxidative stress. To block ROS generation, the cells were pre-incubated with a ROS scavenger (NAC) before the addition of the stress. Fluorescence signal from the cells were either imaged by a confocal laser scanning microscopy (F), or quantified by a fluorometer (G) with an excitation wavelength at 488 nm. The effect of NAC on the NLS cargo transport is included in D. Scale bars: 10 μm .

Oxidative stress differentially regulates influx and efflux rate of importin β through the NPC

We then examined the flux rate of importin β through the NPC, since the accumulation of the cargo in the nucleus depends both on the concentration of RanGTP in the nucleus and on the flux rate of the import complex through the NPC. Purified GFP-fused importin β was incubated with digitonin-treated HeLa nuclei, and the accumulation of fluorescence signal in the nucleoplasm was monitored by time-lapse microscopy (Fig. 2A–C). A detailed kinetic analysis of the fluorescence signal provides both influx and efflux rate constants (k_{in} and k_{out} , respectively) (see also Materials and Methods). In this experimental system, we obtained a k_{out} value that was smaller than the k_{in} (0.15 seconds⁻¹ and 0.0088 seconds⁻¹ for k_{in} and k_{out} in non-stressed cells, respectively), probably because free importin β tends to firmly bind to immobile components within the nucleus (Paradise et al., 2007) and/or RanGTP is depleted from the nucleus, which reduces the apparent efflux rate under microscopic observation.

The k_{in} value was significantly increased (1.4-fold) by DTT treatment of the nuclei, and slightly reduced (0.87-fold) by the oxidative stress (Fig. 2D). DTT treatment restored the effect of oxidative stress and resulted in a higher k_{in} value than seen in the non-stressed cells (Fig. 2D). The k_{out} value was also influenced by DTT and oxidative stress, but in a slightly different way. Oxidative stress significantly reduced the efflux rate by 0.68-fold,

while DTT treatment had little effect (Fig. 2D), implying that the influx and efflux of importin β through the NPC are differently regulated by the redox environment. The pre-treatment of the cells with a ROS scavenger (NAC) before adding the stress significantly reduced the effect of oxidative stress on the influx and efflux (Fig. 2C,D), demonstrating that the flux rate of importin β through the NPC is directly affected by the intracellular ROS.

The passage of non-karyopherin protein was also examined. Proteins smaller than 40 kDa are known to go through the NPC without help of transport mediators (Görllich and Kutay, 1999). When purified hexahistidine (His₆)-tagged GFP (28 kDa) was incubated with the nuclei (stressed or non-stressed), the GFP signal swiftly entered the nucleoplasm and reached to a steady state within 10 minutes. The final concentration in the nucleus was almost the same as that in the external medium (Fig. 2E), suggesting that the passage of GFP is predominantly driven by diffusion. Kinetic analyses of this flux data revealed that the rate constants (k_{in} and k_{out}) were not affected by either oxidative stress or DTT (Fig. 2F).

Oxidative stress induces S–S bond formation in a distinct set of Nups

To examine whether Nups indeed form S–S bonds within the NPC, nuclei were isolated in the absence of DTT from stressed

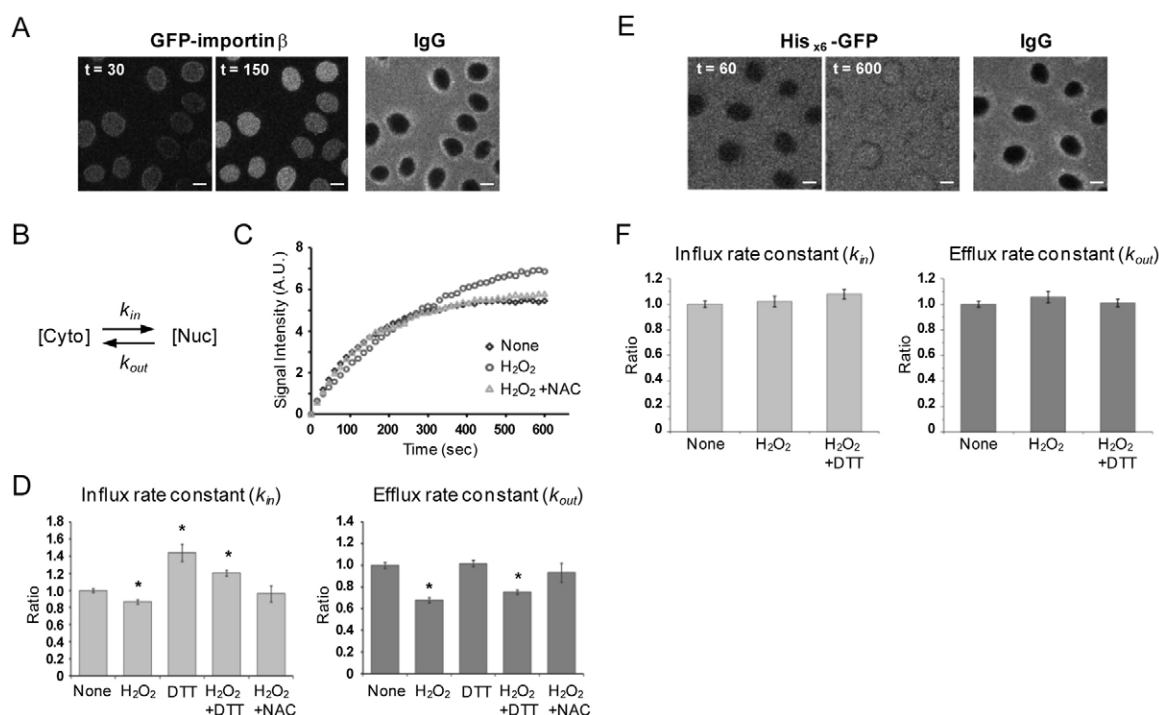


Fig. 2. Oxidative stress reduces the transport rate of importin β but does not affect passive diffusion. HeLa cells were exposed to 0 and 2 mM H₂O₂ and permeabilized with digitonin. Purified GFP-importin β (A–D) or hexahistidine-tagged (His₆)-GFP (E,F) was added together with AlexaFluor568-conjugated IgG, and observed by time-lapse microscopy. (A,E) Fluorescence images of non-stressed cells at indicated times (seconds). The AlexaFluor568-IgG (~150 kDa) signal demonstrates the intact nature of the nuclear envelope. (B) Reaction formula of the transport between the cytoplasm ([Cyto]) and the nucleoplasm ([Nuc]). (C) The fluorescence intensities of GFP-importin β in non-stressed and stressed nuclei in the presence and absence of NAC were plotted against time. Note that at the equilibrium state, the influx rate equals the efflux rate. Therefore, the reduction of the efflux rate constant results in the accumulation of the signal in the nucleus. (D,F) Comparison of k_{in} and k_{out} in the presence and absence of H₂O₂, NAC and DTT treatments. The data from time-lapse observation (represented as in C) was fitted by an exponential curve and the rate constants of influx (k_{in}) and efflux (k_{out}) were determined as described in Materials and Methods. The obtained rate constants were represented by their ratio to those of non-stressed cells. Error bars represent the s.e.m. of measurements from ~40 cells; * P <0.05; Student's t -tests. Scale bars: 10 μ m.

and non-stressed HeLa cells, and analyzed by SDS-PAGE and immunoblotting using Nup-specific antibodies (against Nups 358, 160, 155, 153, 88 and 62) (Fig. 3; the position of each Nup is shown in Fig. 3G). To avoid the oxidation of proteins during the sample preparation, all of the treatments were performed in the presence of the thiol-blocking reagent *N*-ethylmaleimide (NEM, 2 mM). When non-stressed cells (0 mM H_2O_2) were loaded on the gel in the absence of the reducing reagent, the Nup antibodies recognized bands at the expected positions (Fig. 3A–F, asterisks). Several bands (Nups 153, 88 and 160) appeared smear because of the absence of reducing reagent. Careful examination of the immunoreactive bands revealed that Nups 358, 153 and 62 showed additional faint bands with slow migration (Fig. 3A–C; 0 mM H_2O_2 , arrows). Since they disappeared upon DTT treatment, it is speculated that they form S–S bonds in non-stressed cells.

Oxidative stress not only increased the amounts of the slow-migrating bands of Nups 358, 153 and 62, but also induced additional slow-migrating bands of Nups 155, 153 and 62 (Fig. 3A–D; 0.2, 2.0 mM H_2O_2 , arrows). Since these bands completely disappeared upon DTT treatment, they are also derived from S–S bond formation. No DTT-sensitive slow-migrating bands could be detected in Nups 88 and 160 (Fig. 3E,F). The positions of slow-migrating bands vary Nups to Nups, but most of them appear as sharp bands, implying that

distinct numbers and sets of Nups are involved in S–S bond formation. Especially, Nup62 showed more than three additional slow-migrating bands. One of them seems to correspond to dimer (~ 120 kDa), but others are much larger than that. Quantitative analysis of the immunoreactive bands revealed that ~ 41 , 35, 19 and 29% of Nups 358, 155, 153 and 62, respectively formed S–S bonds in 2 mM H_2O_2 . A similar result was obtained from mAb414, which recognizes four different Nups (Nups 358, 214, 153 and 62) (Fig. 4A). mAb414 detected not only the bands of these Nups at the expected positions but also the DTT-sensitive slow-migrating bands in the absence of oxidative stress (Fig. 4A, arrow). In addition, oxidative stress increased the amount of this slow-migrating band and induced an additional slow-migrating band in a concentration-dependent manner (Fig. 4A, arrows). These results are in good agreement with ones from Nups 358, 153 and 62 (Fig. 3A–C).

We performed similar immunoblot analyses with other ROS, including menadione, an oxidative agent like H_2O_2 , and diethylmaleate, a sulfhydryl-reactive agent that has been shown to affect nucleocytoplasmic transport (Crampton et al., 2009; Kodiha et al., 2009; Kodiha et al., 2008; Matsuura and Stewart, 2004; Sato et al., 1993). These reagents also increased the intracellular ROS level as measured by the fluorescent probe (Fig. 1G). As shown in Fig. 4, menadione (Fig. 4B) and diethylmaleate (Fig. 4C) showed an immunoreactive band-pattern

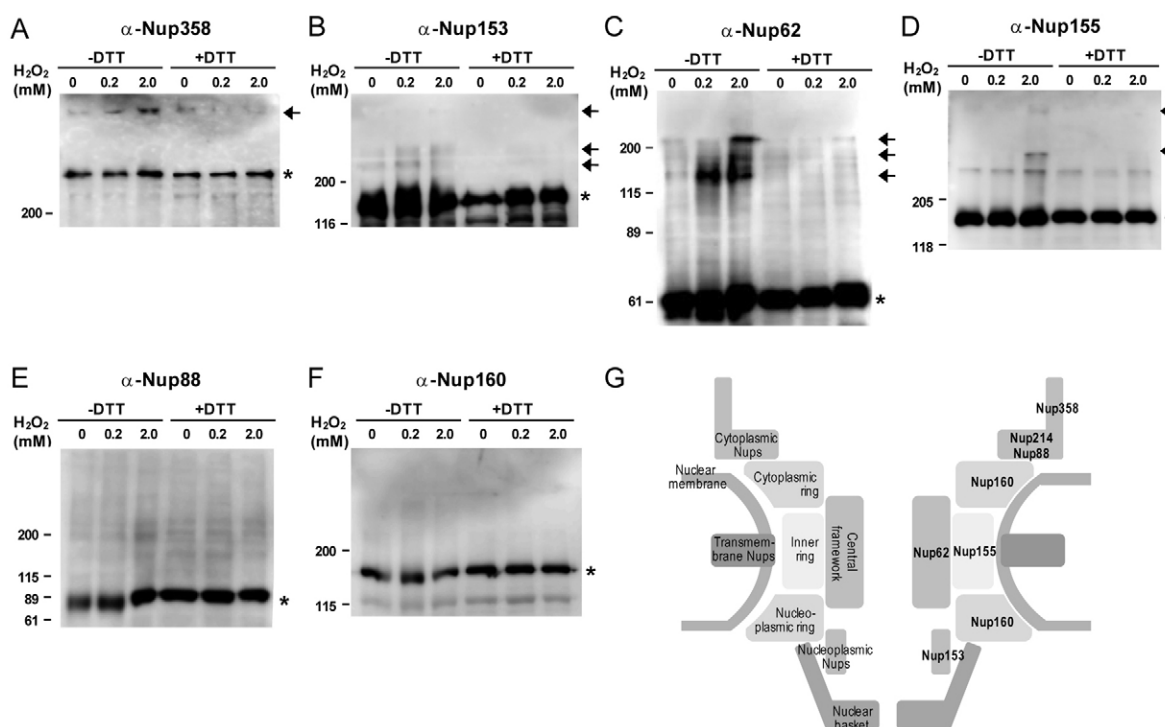


Fig. 3. Oxidative stress promotes S–S bond formation in Nups. (A–F) HeLa cells were exposed to 0, 0.2 and 2.0 mM H_2O_2 and the nuclei collected and prepared for electrophoresis in the absence (–DTT) or presence (+DTT) of 100 mM DTT. The samples were prepared in the presence of NEM to inhibit the formation of S–S bonds during sample preparation. Immunoblot analysis was performed using antibodies against Nup358 (A), Nup153 (B), Nup62 (C), Nup155 (D), Nup88 (E) and Nup160 (F). Slow-migrating bands and bands at the expected positions are indicated by arrows and asterisks, respectively. Nup62 shows a slightly broader (doublet) band in the presence of 2.0 mM H_2O_2 , which is reportedly due to phosphorylation and/or O-glycosylation at certain Ser and/or Thr residues (Crampton et al., 2009). A fast-migrating band could also be detected in Nup62 in the presence of 0.2 mM H_2O_2 . This might be due to an intramolecular S–S bond, which is known to migrate slightly faster than the expected position (Savitsky and Finkel, 2002). Equal loading of protein was confirmed by stripping the blots and re-probing with anti- β -actin antibody (not shown). (G) The localization of Nup subcomplexes within the NPC is illustrated on the basis of a previous report (Brohawn et al., 2009). The Nups analyzed in this study are indicated.

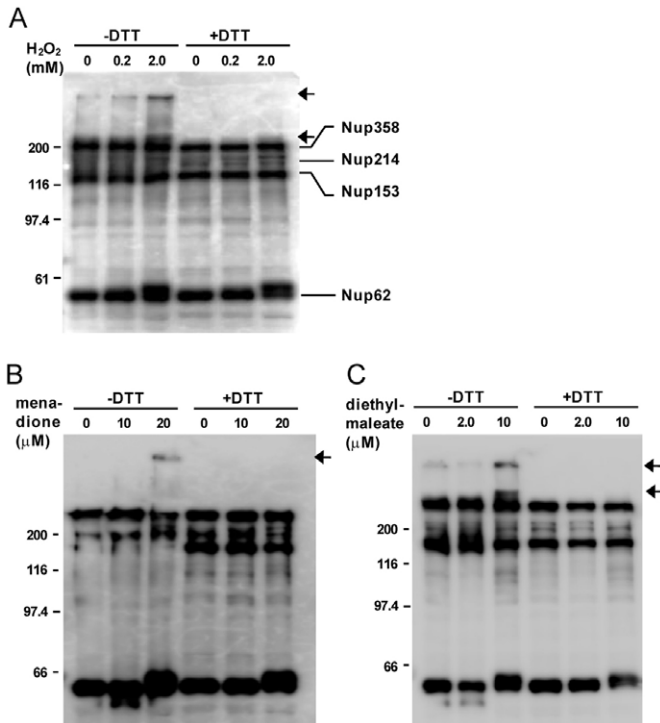


Fig. 4. Other types of ROS also induce S–S bond formation in Nups. HeLa cells were exposed to H_2O_2 (0, 0.2 and 2.0 mM) (A), menadione (0, 10 and 20 μM) (B) or DEM (0, 2.0 and 10 μM) (C) for 1 hour and their nuclei analyzed by immunoblotting with mAb414. The slow-migrating bands are indicated by arrows.

detected by mAb414 similar to that produced by H_2O_2 . These results suggest that the formation of S–S bonds in Nups could be a general response to oxidative stress.

Cysteine residues in Nup62 are directly involved in S–S bond formation and NPC permeability

Nup62 is localized in the central channel of the NPC and plays a crucial role in importin β -dependent nuclear transport (Finlay et al., 1991). The alignment of amino acid sequences of Nup62 revealed two conserved cysteine residues in the C-terminal region (Fig. 5A). We therefore examined whether these cysteine residues form S–S bonds. Hemagglutinin (HA)-tagged Nup62, which carries Cys-to-Ser mutations at these two positions (Fig. 5B), as well as the HA-tagged wild type, were expressed in HeLa cells. The amount of exogenous Nup62 was ~1.5- to 2.0-fold that of the endogenous protein, judging from immunoblotting (data not shown). The existence of slow-migrating bands was examined by western blotting using anti-HA antibody. As is the case in endogenous Nup62 (Fig. 3C), oxidative stress induced the bands at higher positions in non-mutated Nup62; one corresponds to dimer and another is above 200 kDa (Fig. 5C, arrows). In contrast, none of the slow migrating bands was detected in the mutant (Fig. 5C), demonstrating that these cysteine residues are (or at least one of these is) involved in the formation of the DTT-sensitive slow-migrating bands.

The role of cysteine residues in NPC permeability was also examined by an *in vitro* transport assay. HeLa cells overexpressing mutant Nup62 were permeabilized with digitonin and incubated with GFP-fused importin β as described in Fig. 2 (Fig. 5D). Time-lapse

observation of the GFP signal demonstrated that both the influx and efflux rate constants were reduced by the oxidative stress in wild-type-expressing cells, whereas none of them was affected in mutant-expressing cells (Fig. 5E). The influx rate of the wild-type was increased by pre-treatment with DTT as is the case in non-transfected HeLa cells (Fig. 2D), whereas the mutant did not exhibit a DTT-sensitive influx rate (Fig. 5E). These results clearly demonstrated that S–S bond formation in Nup62 directly affects the transport of importin β . The export rate was not significantly increased upon DTT treatment (Fig. 5E), suggesting that some modifications in the cysteine residues other than S–S bonds regulate the export of importin β . This result, as well as Fig. 2D, supports the idea that the influx and efflux through the NPC can be independently regulated (see Discussion).

The transport rate of NLS cargo by importin α/β pathway was also examined by the cells overexpressing mutant Nup62. As shown in Fig. 5F, the influx rate of NLS cargo was reduced by oxidative stress in the case of wild-type expressing cells, but less affected in mutant-expressing cells. This is consistent with the fact that the influx rate of importin β was reduced by the stress in wild-type Nup62 but not affected by the stress in mutant Nup62 (Fig. 5E). These results all demonstrated that stress-induced S–S bond formation of Nup62 affects the passage of importin β and also importin- α/β -dependent cargo transport.

Different types of Nups form intermolecular S–S bridges

When Nup62 was knocked down by siRNA and then the cells were exposed to oxidative stress followed by western blot analysis, the immunoreactive bands for Nup62 were decreased to 48% of those seen in control cells (Fig. 6A,B). Namely, the amounts of monomer (Fig. 6A, asterisk), as well as the slow-migrating populations, were reduced in the knockdown cells. When the same nuclei were analyzed with anti-Nup358 and 153 antibodies, the immunoreactive bands were not affected (Fig. 6C,D). However, in the case of Nup155, two of the slow-migrating bands significantly decreased in Nup62 knockdown cells (Fig. 6C, arrows and Fig. 6D). The knockdown of Nup153 did not affect the slow-migrating bands of Nups 358 and 62 (Fig. 6E,F). These results suggest that Nups 155 and 62 are covalently crosslinked via S–S bonds in the presence of oxidative stress, whereas Nups 358 and 153 form S–S bonds within the same type of Nup. It should be noted that immunoblotting for Nup62 and Nup155 revealed slow-migrating bands at the same positions (Fig. 3C,D, arrows).

Discussion

In this study, we demonstrated that NPC contains a significant amount of S–S bonds which are sensitive to oxidative stress, and that these S–S bonds are directly involved in the regulation of importin β -dependent nuclear transport. The results obtained here imply that the S–S bond is one of the fundamental determinants of the properties of the NPC channel. The fact that Nups form S–S bonds even in the absence of oxidative stress suggests that endogenous ROS and reducing reagents can be regulators of nuclear transport.

Stress-dependent and independent S–S bond formation within Nups

The central channel of the NPC is filled with flexible polypeptide chains of Nups which carry a number of phenylalanine residues (FG-Nups) (Bayliss et al., 2000; Ben-Efraim and Gerace, 2001; Peters, 2009; Strawn et al., 2004; Terry and Wente, 2007). It has been proposed that the flexible polypeptide chains of FG-Nups

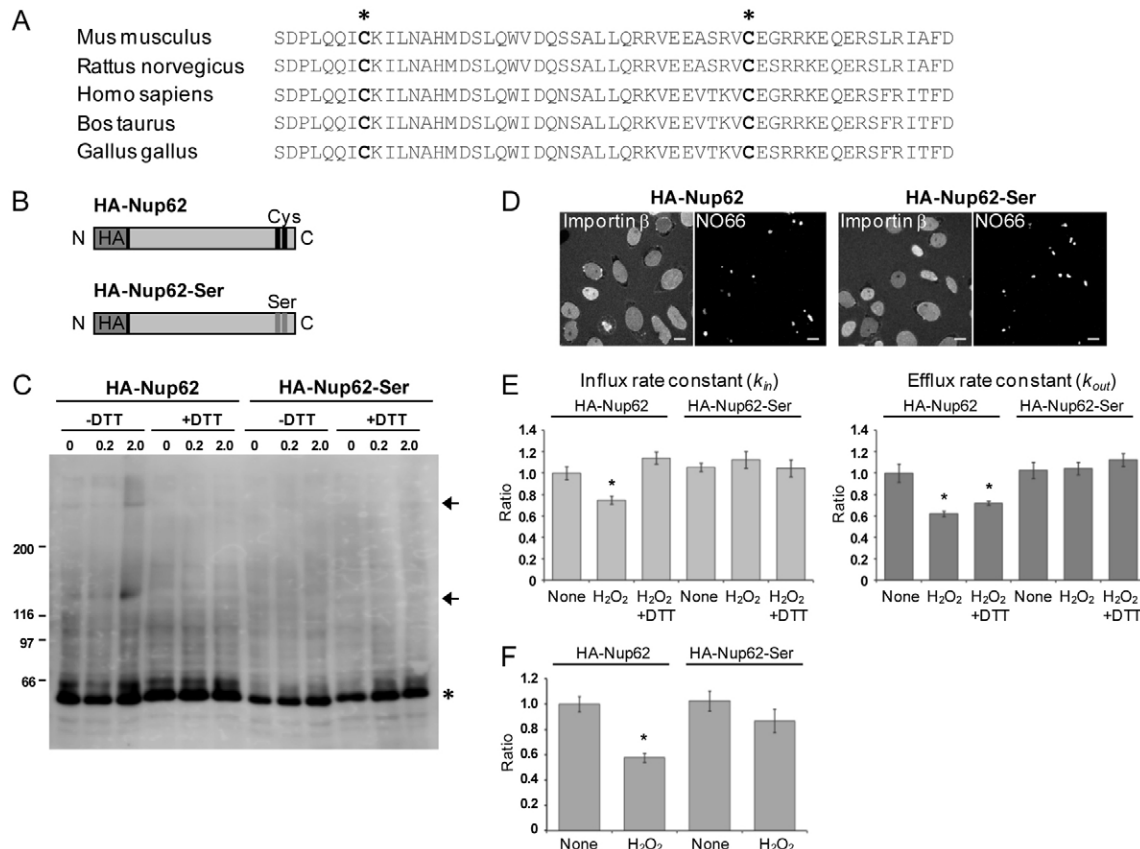


Fig. 5. Two cysteine residues in Nup62 are involved in S-S bond formation and NPC permeability. (A) The amino acid sequences of the C-termini of Nup62 from different species are shown. Cysteine residues are marked with asterisks. (B) Scheme of hemagglutinin-tagged Nup62 (HA-Nup62) and Nup62 containing the point mutations C478S and C509S (HA-Nup62-Ser). (C) HeLa cells expressing HA-Nup62 and HA-Nup62-Ser were treated with H₂O₂ (0, 0.2 and 2.0 mM) and their nuclei analyzed by immunoblotting with anti-HA antibody. The bands are indicated by arrows and asterisks as in Fig. 3. The stress-inducible other modifications that can be observed in Fig. 3C could not be detected, implying that these modifications occur in a limited fraction of Nup62. (D,E) Time-lapse imaging of GFP-importin β was performed using permeabilized HeLa cells that transiently expressed HA-Nup62 or HA-Nup62-Ser and had been exposed to 2.0 mM H₂O₂. (D) Fluorescence images of cells 150 seconds after the addition of GFP-importin β . mRFP-NO66 is an expression marker of HA-Nup62 (left) and HA-Nup62-Ser (right). (E) Comparison of k_{in} and k_{out} in cells expressing HA-Nup62 and HA-Nup62-Ser in the presence and absence of H₂O₂ and DTT treatment. Rate constants are represented in terms of their ratio to those of HA-Nup62-expressing cells without H₂O₂ and DTT treatment. Error bars represent the s.e.m. of measurements from ~10 cells. (F) The import assay of NLS cargo was performed using the nuclei expressing HA-Nup62 and HA-Nup62-Ser as described in Fig. 1C; * $P < 0.01$; Student's t -tests. Scale bars: 10 μ m.

form a meshwork via hydrophobic interactions between hydrophobic residues (mainly phenylalanine) (Frey et al., 2006; Mohr et al., 2009; Moussavi-Baygi et al., 2011; Ribbeck and Görlich, 2002). This meshwork prevents the passage of large proteins, but allows diffusion of proteins smaller than the mesh size (Mohr et al., 2009). Karyopherins are able to migrate in this hydrophobic meshwork because of their hydrophobic characteristics. The S-S bonds among these Nups could change the characteristics of the meshwork; intermolecular covalent crosslinking of polypeptides could reduce the flexibility of the meshwork and hence the permeability of karyopherins.

Immunoblot analysis indicated that the amount of S-S bonds significantly increased upon the addition of the stress (Nups 358, 155, 153 and 62), although a small amount could be detected in the absence of the stress (Nups 358, 153 and 62) (Fig. 3). Therefore, H₂O₂-dependent reduction of transport is due to S-S bond formation in these Nups. It should be noted that Nup62, a component of the central channel of the NPC, has been demonstrated to be a stress sensor, and phosphorylated and

glycosylated upon exposure to cellular stresses (Crampton et al., 2009; Miller et al., 1999). Therefore, S-S bond formation and the concomitant reduction of nuclear transport is one of the mechanisms of Nup62-dependent stress responses. The presence of the S-S bonds of Nups 358, 153 and 62 even in the absence of the stress imply that they might be one of the fundamental components of the hydrophobic meshwork in the NPC. In good agreement with this is the effect of DTT to the non-stressed cells (Figs 1E and 2D); the treatment of non-stressed nuclei with DTT slightly increased the nuclear import of the NLS cargo and influx rate of importin β . The fact that DTT treatment enhanced the flux rate of importin β but not that of GFP (Fig. 2) suggests that the minimum size of the mesh is not affected by S-S bridging.

Nup positioning within the NPC and S-S bond formation

Our knockdown experiments using siRNA imply that Nup62 and Nup155 are crosslinked via S-S bond(s) (Fig. 6). This is a reasonable result since Nups 62 and 155 exist in the central part

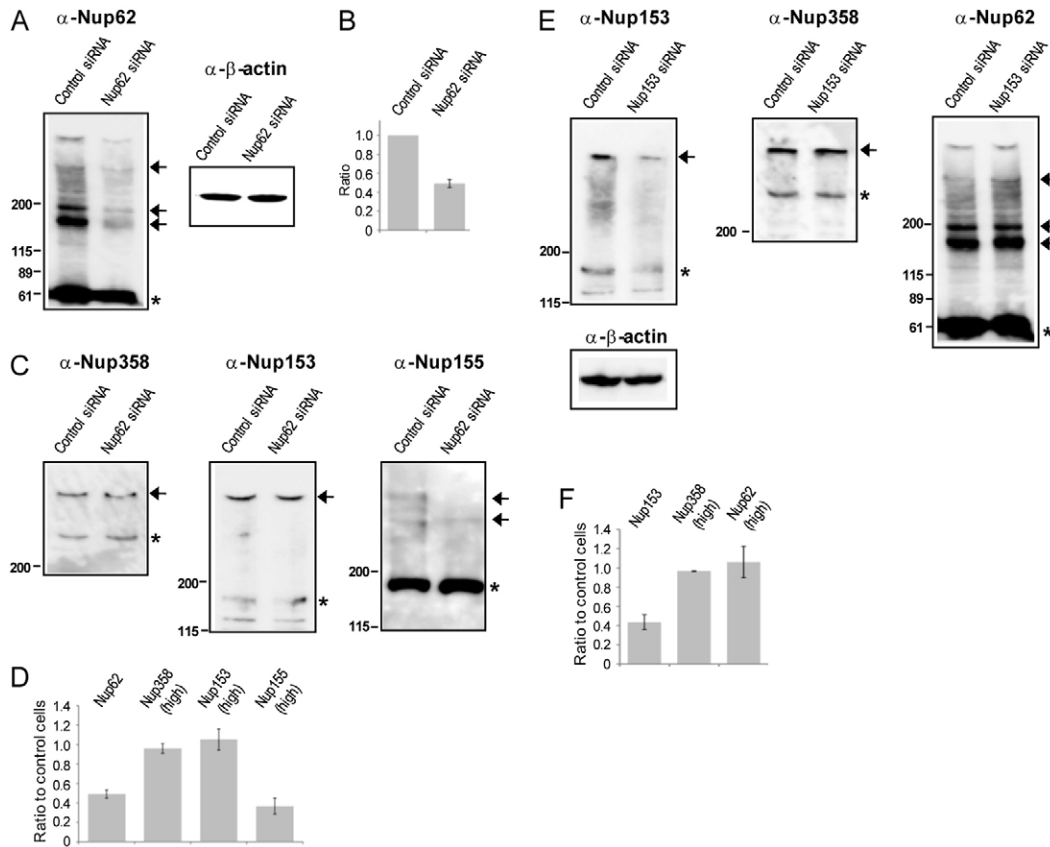


Fig. 6. Nup depletion by RNAi affects some of the stress-inducible bands. HeLa cells were transfected with siRNA against Nup62 (A–D) and Nup153 (E–F) and exposed to 2.0 mM H_2O_2 . Nuclei were subjected to immunoblot analysis. siRNA against luciferase was used as a negative control. (A,C,E) Immunoblot analysis of isolated nuclei using anti-Nup62, 358, 153 and 155 antibodies; anti- β -actin antibody was a loading control. The bands are indicated by arrows and asterisks as in Fig. 3. (B,D,F) The intensities of the Nup62 band (B) and of the high molecular weight bands of Nups 62, 358, 153 and 155 (D,F) were quantified and presented in terms of their ratio to the values seen in control cells. Error bars represent s.e.m. from at least three independent experiments.

of the NPC and are supposed to be relatively close to each other (Fig. 3G). On the other hand, knockdown of Nup153 (existing in the nucleoplasmic side of the NPC) did not affect the slow-migrating bands of Nups 358 and 62 (Fig. 6E), suggesting that Nup153 does not form S–S bonds with these Nups. Immunoblot analysis with anti-Nup62 antibody revealed several slow-migrating bands at 120–200 kDa (Fig. 3C). These bands could be either a homomultimer of Nup62 or a heteromultimer with other Nups. The most plausible partners of heteromultimer could be Nups 58, 54 and 45, all of which are known to make a complex with Nup62 (Nup62 complex) (Solmaz et al., 2011; Stoffler et al., 1999). Nups in the Nup93 subcomplex (Nups 205, 188, 155, 93 and 35) are also candidates, since the Nup62 complex is anchored to the Nup93 subcomplex (Grandi et al., 1997; Krull et al., 2004; Sachdev et al., 2012). Further study will be required to elucidate the S–S network among Nups.

We could not find any clear relationship between the formation of S–S bonds and the number of conserved cysteine residues (39 residues in Nup358, 17 in Nup153, 2 in Nup62, 20 in Nup155, 27 in Nup160, and 19 in Nup88; supplementary material Fig. S1). This means that S–S bonds do not form in random positions, but rather form between distinct sets of Nups. Neighboring amino acid sequences, higher-order architectures, and/or spatial locations in the NPC may decide which cysteine residues are to be involved in S–S bond formation. A previous study has

demonstrated that a basic amino acid adjacent to a cysteine residue increases the reactivity of the thiol group (Winterbourn and Hampton, 2008). Indeed, there are several basic amino acids around the two cysteine residues of Nup62 (Fig. 5A). Nups 358, 153 and 155 also contain several cysteine residues just adjacent to either lysine or arginine (18 out of 77 cysteines in Nup358, 9 out of 28 in Nup153, 3 out of 28 in Nup155). These cysteine residues could be the targets of S–S bridging.

Are influx and efflux through the NPC differently regulated?

Our kinetic analysis showed that while oxidative stress influenced both the influx and efflux of importin β , DTT treatment affected only the influx but not the efflux (Fig. 2D; Fig. 5E). This implies that oxidative stress regulates the efflux via mechanisms other than S–S bond formation. Previous studies have demonstrated that Nups 214, 153, 98, 88 and 62 are phosphorylated and/or glycosylated by oxidative stress (Crampton et al., 2009; Kodiha et al., 2009). Other studies have reported that the Nup214/Nup88 complex and Nup98 are involved in export but not in import (Hutten and Kehlenbach, 2006; Oka et al., 2010). Therefore, it might be the case that phosphorylation and glycosylation in these Nups inhibit export but not import. Other possibility is that NPCs may not be homogeneous. Recent studies utilizing super-resolution fluorescence microscopy reported that the Nup composition of the NPC (Nup214 and Nup62) varies between individual NPCs within

a single mammalian cell (Kinoshita et al., 2012). Oxidative stress might introduce different kinds of modifications into distinct NPCs, resulting in differential regulation of import and export. Alternatively, oxidative stress might increase the affinities of some factors in the nucleus to importin β , which would result in the reduction of efflux in stressed cells.

The NPC channel has a redox environment distinct from that of the cytoplasm

In this report, we show a line of evidence for the direct regulation of a cellular function by S–S bonds. Recently it has been reported that S–S bond formation within Lamin A, a scaffold protein of the nuclear envelope, plays an important role in tolerance to ROS and preventing cells from senescence (Pekovic et al., 2011). Since nuclear transport is tightly linked to the entire intracellular signaling pathway, S–S bond formation within the NPC would also contribute to cellular homeostasis.

Cysteine modifications have so far been known to regulate protein function via one or several of the following mechanisms: (i) modification of a thiol group in the catalytic center directly changes the enzymatic activity of the protein, (ii) thiol modification produces an allosteric effect on the enzyme, and (iii) thiol modification alters interactions with other proteins (Jones, 2008). The S–S bonds within the NPC do not seem to belong to any of these mechanisms, and therefore may represent a novel mechanism for the regulation of protein function. The cytoplasm is normally maintained in a reducing state due to ubiquitous reducing reagents such as glutathione. Our results shown here imply that the inner channel of the NPC is in a different redox environment from the cytoplasm (more oxidative), and may be more sensitive to oxidative stress and intracellular reducing reagents than the cytoplasm.

Materials and Methods

Cell culture and oxidative stress

HeLa S3 cells (ATCC, CCL-2.2) were cultured in Dulbecco's Modified Eagle's Medium (DMEM) (Sigma, St. Louis, MO) with 10% fetal bovine serum (FBS). Cells were treated with H₂O₂ (0.1–2.0 mM), menadione (10 μ M and 20 μ M), and diethylmaleate (2.0 μ M and 10 μ M) for 1 hour. The generation of ROS was blocked by the pre-treatment of cells with 10 mM *N*-acetyl cysteine (NAC) (Nacalai Tesque, Kyoto, Japan) for 1 hour before the addition of H₂O₂.

Antibodies

Antibodies against Nups were purchased from the following companies; mAb414 (Covance, in Princeton, NJ), anti-Nup358 (Affinity BioReagents, Golden, CO), anti-Nup153 (Immunoquest, Baltimore, MD), anti-Nup62 (BD Biosciences, Franklin Lakes, NJ), and anti-Nup160, 88 (Santa Cruz Biotechnology, Santa Cruz, CA). A rabbit polyclonal anti-Nup155 antibody is a kind gift from Dr Mattaj (European Molecular Biology Laboratory) (Franz et al., 2005). Anti- β -actin antibody and anti-Ran antibody (clone 20) were purchased from Sigma and BD Biosciences, respectively. For the detection of Nup160 and Nup153, biotinylated anti-sheep/goat antibody (GE Healthcare, Little Chalfont, UK) and streptavidin-conjugated horseradish peroxidase (HRP)-coupled antibody (GE Healthcare) were used. In other cases, HRP-coupled secondary antibodies against mouse (GE Healthcare), rabbit (GE Healthcare), or goat (Cappel Laboratories, Malvern, PA) were used.

Plasmids, cDNAs and protein expression

The cDNA of rat Nup62 (Otsuka et al., 2008) was subcloned into the expression vector pcDNA3.1 (Invitrogen, Carlsbad, CA) with an HA tag at the N-terminus. Site-directed mutagenesis of Nup62 was performed using the GeneTailor Site-Directed Mutagenesis system (Invitrogen). cDNA encoding human NO66 was amplified from the cDNA pool of HeLa cells by PCR and inserted into a vector in which the EGFP coding region in the pEGFP-C1 vector (Invitrogen) is replaced by the cDNA of mRFP (a kind gift from Dr Yoneda, Osaka University). The plasmids were introduced into HeLa cells with the transfection reagent, Effectene (Qiagen, Valencia, CA), according to the manufacturer's protocol. Recombinant proteins (importin α 1, importin β 1, Ran, and GFP) were expressed in *E. coli* cells

(BL21-CodonPlus(DE3)-RIL, Agilent Technologies, Wilmington, DE) as affinity-tagged fusion proteins (GST or His₆) and affinity purified as described previously (Kumeta et al., 2010; Yoshimura et al., 2006). As for GST-fused proteins, proteins were cleaved from GST by protease digestion, if necessary (Otsuka et al., 2008). We generated siRNAs against Nup62 (Hubert et al., 2009) and Nup153 (Harborth et al., 2001) by using an *in vitro* transcription kit (Takara, Shiga, Japan). The siRNAs against luciferase were purchased from Invitrogen. HeLa cells were transfected with siRNA using Lipofectamine 2000 (Invitrogen) 45–50 hours before the immunoblot analysis.

Quantification of intracellular ROS

The intracellular ROS was quantitated by using ROS-reactive fluorescence probe as described in the previous study (Pekovic et al., 2011). HeLa cells were cultured in DMEM without phenol red and supplemented with 10% FBS. Carboxyl-H₂DCFDA (5-(and-6)-carboxy-2',7'-dichlorodihydrofluorescein diacetate, Invitrogen, Carlsbad, CA) was added to the culture medium at a final concentration of 10 μ M, and incubated for 1 hour at 37°C. The cells were observed under the fluorescence microscope equipped with a stage heater. H₂O₂ was added to the culture medium and microscopic observation was continued up to 1 hour. To block the generation of ROS, 10 mM NAC was also added to the culture medium during the pre-incubation time. The cells were then exposed to the oxidative stress and harvested after one hour. The cells were washed three times with phosphate-buffered saline (PBS) and the fluorescence signal was measured with an excitation wavelength at 488 nm.

Immunostaining for digitonin-treated HeLa cells

HeLa cells were washed twice with transport buffer (TB; 20 mM HEPES, pH 7.3, 110 mM potassium acetate, 5 mM sodium acetate, 2 mM magnesium acetate, and 1 mM EGTA), permeabilized by TB containing 40 μ g/ml digitonin for 5 minutes on ice, washed twice with TB, incubated with TB at 37°C for 10 minutes, and washed twice with TB. Cells were then fixed with 4% paraformaldehyde and immunostained with anti-Ran antibody and fluorescein isothiocyanate-conjugated anti-mouse IgG (Cappel Laboratories) as described in the previous report (Kumeta et al., 2010).

Immunoblotting for purified nuclei

For immunoblotting in Fig. 1, HeLa cells were washed twice with TB, permeabilized by TB containing 40 μ g/ml digitonin for 5 minutes on ice, washed twice with TB, incubated with TB at 37°C for 10 minutes, and washed twice with TB. Digitonin-treated or non-treated cells were harvested and collected by centrifugation (700 \times g for 2 minutes), suspended in sample buffer, boiled with 100 mM DTT, and subjected to SDS-PAGE and western blotting. Ran and histone H3 were detected using anti-Ran antibody (C-20, Santa Cruz Biotechnology) and anti-histone H3 antibody (Upstate Biotechnology, Lake Placid, NY), respectively. For immunoblotting experiments in Figs 3–5, HeLa cells (with or without oxidative stress) were washed twice with PBS, harvested by a scraper, and collected by centrifugation (700 \times g for 2 minutes). The cells were permeabilized by a treatment with 40 μ g/ml digitonin in PBS containing 2 mM *N*-ethylmaleimide (NEM) (Nacalai Tesque, Kyoto, Japan) for 5 minutes and the nuclei were separated from cytosolic components by centrifugation (700 \times g for 2 minutes). The isolated nuclei were further incubated with PBS containing 0.5% Triton X-100 and 2 mM NEM for 5 minutes and soluble nucleoplasmic proteins were removed by centrifugation (700 \times g for 2 minutes). All steps were carried out at 4°C. Finally, the enriched nuclei were suspended in the sample buffer, boiled for 5 minutes with or without 100 mM DTT, and subjected to SDS-PAGE followed by immunoblot detection. For immunoblotting in Fig. 6, the digitonin and Triton X-100 treatment was performed without NEM. The amount of slow-migrating band at 2 mM H₂O₂ was quantitated in each Nup. In immunoblotting, the transfer efficiency of a protein band to the blotting membrane varies depending on the molecular weight of the protein; larger proteins are less transferable to the membrane. Therefore, the fraction(s) of slow-migrating band(s) in the total amount of each subunit was estimated by subtracting the band intensity at the expected position (asterisk) in the absence of DTT from that in the presence, by using non-saturating immunoblot signals.

In vitro transport assay

The transport assay was performed as described in previous reports (Kumeta et al., 2012; Kumeta et al., 2010), except that digitonin-treated cells were pre-incubated with or without DTT for 10 minutes at 37°C before the addition of fluorescent proteins. For the transport assay of NLS cargo, the cells were incubated with 4 μ M importin α , 4 μ M importin β , 25 μ M His₆-RanGDP, 2.5 μ M GST-NLS-GFP, and ATP regeneration system (1 mM ATP, 5 mM creatine phosphate and 200 U/ml creatine phosphokinase) at room temperature for 5 minutes. The cells were then fixed with 4% paraformaldehyde and observed by confocal microscopy (LSM 5 PASCAL; Zeiss, Oberkochen, Germany). For time-lapse observation of NPC permeability in Fig. 2, 0.5 μ M His₆-GFP or GFP-fused importin β was applied to digitonin-treated cells together with Alexa-Fluor-568-conjugated IgG (Invitrogen), and observed by confocal microscopy (LSM510; Zeiss). Images were collected

every 10 seconds for 10 minutes for His₆-GFP and every 5 seconds for 5 minutes for GFP-importin β . The image of Alexa-Fluor-IgG was taken after the time-lapse observation. The mean nuclear fluorescence intensity was quantified by the Zeiss LSM software. For the time-lapse experiment in Fig. 5, 1.0 μ M GFP-importin β was added to permeabilized cells and observed using confocal microscopy (LSM 5 PASCAL). Images were collected every 12 seconds. The image of mRFP-NO66 (transfection marker) was taken after time-lapse observation. The fluorescence intensity was measured only in cells expressing mRFP-NO66.

Kinetic analysis of nuclear transport

The rate of protein influx from the cytoplasm to the nucleoplasm can be expressed using the following equation:

$$d[\text{Nuc}]/dt = k_{in}[\text{Cyt}] - k_{out}[\text{Nuc}], \quad (1)$$

where [Nuc] and [Cyt] are the concentrations of GFP-fused proteins in the nucleoplasm and in the cytoplasm, respectively, and k_{in} and k_{out} are the rate constants of influx and efflux, respectively. In the *in vitro* transport assay using permeabilized cells, [Cyt] corresponds to the substrate concentration in the chamber, which is constant throughout the measurement. Therefore, Eq. 1 can be converted to:

$$[\text{Nuc}] = k_{in}[\text{Cyt}]/k_{out}\{1 - \exp(-k_{out}t)\}. \quad (2)$$

The average fluorescence intensity of each nucleus was measured and plotted against time, and fitted with Eq. 2 to obtain k_{in} and k_{out} .

Acknowledgements

We thank Dr Yoneda (Osaka University) for his kind gift of cDNAs encoding importin α and β , Dr Ullman (Utah University) for the cDNA encoding Nup62, Dr Horigome (Niigata University) for the cDNA encoding Ran and Dr Mattaj (European Molecular Biology Laboratory) for an antibody against Nup155. We thank Y. Takashima and K. Ogawa for their technical assistance.

Author contributions

S.O., M.T. and S.H.Y. performed all experiments and analyses. S.O. and S.H.Y. designed the study. S.O., S.H.Y., K.M. and K.T. discussed the results and wrote the paper.

Funding

This study was financially supported by a Funding Program for Next Generation World-leading Researchers (S.H.Y.), a Grant-in-Aid for Scientific Research (B) (S.H.Y.), a Grant-in-Aid for Young Scientists (A) (S.H.Y.), and a Grant-in-Aid for Scientific Research on Priority Areas ('Bio-manipulation' for S.H.Y.) from the Japan Society for the Promotion of Science (JSPS), and a Grant-in-Aid for Scientific Research on Innovative Areas ('Spying minority in biological phenomena' for M.K. and 'RNA biofunctions and viruses' for K.T.) from the Ministry of Education, Culture, Sports, Science and Technology, Japan. S.O. is a recipient of the JSPS fellowships [research fellowship for young scientists (DC1) and postdoctoral fellowship for research abroad].

Supplementary material available online at

<http://jcs.biologists.org/lookup/suppl/doi:10.1242/jcs.124172/-/DC1>

References

- Bayliss, R., Littlewood, T. and Stewart, M. (2000). Structural basis for the interaction between FxFG nucleoporin repeats and importin-beta in nuclear trafficking. *Cell* **102**, 99-108.
- Ben-Efraim, I. and Gerace, L. (2001). Gradient of increasing affinity of importin beta for nucleoporins along the pathway of nuclear import. *J. Cell Biol.* **152**, 411-417.
- Brohawn, S. G., Partridge, J. R., Whittle, J. R. and Schwartz, T. U. (2009). The nuclear pore complex has entered the atomic age. *Structure* **17**, 1156-1168.
- Crampton, N., Kodiha, M., Shrivastava, S., Umar, R. and Stochaj, U. (2009). Oxidative stress inhibits nuclear protein export by multiple mechanisms that target FG nucleoporins and Crm1. *Mol. Biol. Cell* **20**, 5106-5116.
- Finlay, D. R., Meier, E., Bradley, P., Horecka, J. and Forbes, D. J. (1991). A complex of nuclear pore proteins required for pore function. *J. Cell Biol.* **114**, 169-183.
- Franz, C., Askjaer, P., Antonin, W., Iglesias, C. L., Haselmann, U., Schelder, M., de Marco, A., Wilm, M., Antony, C. and Mattaj, I. W. (2005). Nup155 regulates nuclear envelope and nuclear pore complex formation in nematodes and vertebrates. *EMBO J.* **24**, 3519-3531.
- Frey, S., Richter, R. P. and Görlich, D. (2006). FG-rich repeats of nuclear pore proteins form a three-dimensional meshwork with hydrogel-like properties. *Science* **314**, 815-817.
- Görlich, D. and Kutay, U. (1999). Transport between the cell nucleus and the cytoplasm. *Annu. Rev. Cell Dev. Biol.* **15**, 607-660.
- Grandi, P., Dang, T., Pané, N., Shevchenko, A., Mann, M., Forbes, D. and Hurt, E. (1997). Nup93, a vertebrate homologue of yeast Nup96, forms a complex with a novel 205-kDa protein and is required for correct nuclear pore assembly. *Mol. Biol. Cell* **8**, 2017-2038.
- Harborth, J., Elbashir, S. M., Bechert, K., Tuschl, T. and Weber, K. (2001). Identification of essential genes in cultured mammalian cells using small interfering RNAs. *J. Cell Sci.* **114**, 4557-4565.
- Hubert, T., Vandekerckhove, J. and Gettemans, J. (2009). Exo70-mediated recruitment of nucleoporin Nup62 at the leading edge of migrating cells is required for cell migration. *Traffic* **10**, 1257-1271.
- Hutten, S. and Kehlenbach, R. H. (2006). Nup214 is required for CRM1-dependent nuclear protein export in vivo. *Mol. Cell Biol.* **26**, 6772-6785.
- Jones, D. P. (2008). Radical-free biology of oxidative stress. *Am. J. Physiol. Cell Physiol.* **295**, C849-C868.
- Kinoshita, Y., Kalir, T., Dottino, P. and Kohtz, D. S. (2012). Nuclear distributions of NUP62 and NUP214 suggest architectural diversity and spatial patterning among nuclear pore complexes. *PLoS ONE* **7**, e36137.
- Kobayashi, A., Kang, M. I., Watai, Y., Tong, K. I., Shibata, T., Uchida, K. and Yamamoto, M. (2006). Oxidative and electrophilic stresses activate Nrf2 through inhibition of ubiquitination activity of Keap1. *Mol. Cell Biol.* **26**, 221-229.
- Kodiha, M., Chu, A., Matusiewicz, N. and Stochaj, U. (2004). Multiple mechanisms promote the inhibition of classical nuclear import upon exposure to severe oxidative stress. *Cell Death Differ.* **11**, 862-874.
- Kodiha, M., Tran, D., Qian, C., Morogan, A., Presley, J. F., Brown, C. M. and Stochaj, U. (2008). Oxidative stress mislocalizes and retains transport factor importin-alpha and nucleoporins Nup153 and Nup88 in nuclei where they generate high molecular mass complexes. *Biochim. Biophys. Acta* **1783**, 405-418.
- Kodiha, M., Tran, D., Morogan, A., Qian, C. and Stochaj, U. (2009). Dissecting the signaling events that impact classical nuclear import and target nuclear transport factors. *PLoS ONE* **4**, e8420.
- Krull, S., Thyberg, J., Björkroth, B., Rackwitz, H. R. and Cordes, V. C. (2004). Nucleoporins as components of the nuclear pore complex core structure and Tpr as the architectural element of the nuclear basket. *Mol. Biol. Cell* **15**, 4261-4277.
- Kumeta, M., Yoshimura, S. H., Harata, M. and Takeyasu, K. (2010). Molecular mechanisms underlying nucleocytoplasmic shuttling of actinin-4. *J. Cell Sci.* **123**, 1020-1030.
- Kumeta, M., Yamaguchi, H., Yoshimura, S. H. and Takeyasu, K. (2012). Karyopherin-independent spontaneous transport of amphiphilic proteins through the nuclear pore. *J. Cell Sci.* **125**, 4979-4984.
- Matsuura, Y. and Stewart, M. (2004). Structural basis for the assembly of a nuclear export complex. *Nature* **432**, 872-877.
- Mattaj, I. W. and Englmeier, L. (1998). Nucleocytoplasmic transport: the soluble phase. *Annu. Rev. Biochem.* **67**, 265-306.
- Miller, M. W., Caracciolo, M. R., Berlin, W. K. and Hanover, J. A. (1999). Phosphorylation and glycosylation of nucleoporins. *Arch. Biochem. Biophys.* **367**, 51-60.
- Miyamoto, Y., Saiwaki, T., Yamashita, J., Yasuda, Y., Kotera, I., Shibata, S., Shigeta, M., Hiraoka, Y., Haraguchi, T. and Yoneda, Y. (2004). Cellular stresses induce the nuclear accumulation of importin alpha and cause a conventional nuclear import block. *J. Cell Biol.* **165**, 617-623.
- Mohr, D., Frey, S., Fischer, T., Güttler, T. and Görlich, D. (2009). Characterisation of the passive permeability barrier of nuclear pore complexes. *EMBO J.* **28**, 2541-2553.
- Mosammaparast, N. and Pemberton, L. F. (2004). Karyopherins: from nuclear-transport mediators to nuclear-function regulators. *Trends Cell Biol.* **14**, 547-556.
- Motohashi, H. and Yamamoto, M. (2004). Nrf2-Keap1 defines a physiologically important stress response mechanism. *Trends Mol. Med.* **10**, 549-557.
- Moussavi-Baygi, R., Jamali, Y., Karimi, R. and Mofrad, M. R. (2011). Brownian dynamics simulation of nucleocytoplasmic transport: a coarse-grained model for the functional state of the nuclear pore complex. *PLOS Comput. Biol.* **7**, e1002049.
- Oka, M., Asally, M., Yasuda, Y., Ogawa, Y., Tachibana, T. and Yoneda, Y. (2010). The mobile FG nucleoporin Nup98 is a cofactor for Crm1-dependent protein export. *Mol. Biol. Cell* **21**, 1885-1896.
- Otsuka, S., Iwasaka, S., Yoneda, Y., Takeyasu, K. and Yoshimura, S. H. (2008). Individual binding pockets of importin-beta for FG-nucleoporins have different binding properties and different sensitivities to RanGTP. *Proc. Natl. Acad. Sci. USA* **105**, 16101-16106.
- Paradise, A., Levin, M. K., Korza, G. and Carson, J. H. (2007). Significant proportions of nuclear transport proteins with reduced intracellular mobilities resolved by fluorescence correlation spectroscopy. *J. Mol. Biol.* **365**, 50-65.
- Patel, V. P., Defranco, D. B. and Chu, C. T. (2012). Altered transcription factor trafficking in oxidatively-stressed neuronal cells. *Biochim. Biophys. Acta* **1822**, 1773-1782.
- Pekovic, V., Gibbs-Seymour, I., Markiewicz, E., Alzoughaibi, F., Benham, A. M., Edwards, R., Wenhert, M., von Zglinicki, T. and Hutchison, C. J. (2011). Conserved cysteine residues in the mammalian lamin A tail are essential for cellular responses to ROS generation. *Aging Cell* **10**, 1067-1079.

- Peters, R.** (2009). Translocation through the nuclear pore: Kaps pave the way. *Bioessays* **31**, 466-477.
- Rhee, S. G., Kang, S. W., Jeong, W., Chang, T. S., Yang, K. S. and Woo, H. A.** (2005). Intracellular messenger function of hydrogen peroxide and its regulation by peroxiredoxins. *Curr. Opin. Cell Biol.* **17**, 183-189.
- Ribbeck, K. and Görlich, D.** (2002). The permeability barrier of nuclear pore complexes appears to operate via hydrophobic exclusion. *EMBO J.* **21**, 2664-2671.
- Sachdev, R., Sieverding, C., Flötenmeyer, M. and Antonin, W.** (2012). The C-terminal domain of Nup93 is essential for assembly of the structural backbone of nuclear pore complexes. *Mol. Biol. Cell* **23**, 740-749.
- Sato, H., Ishii, T., Sugita, Y., Tateishi, N. and Bannai, S.** (1993). Induction of a 23 kDa stress protein by oxidative and sulphydryl-reactive agents in mouse peritoneal macrophages. *Biochim. Biophys. Acta* **1148**, 127-132.
- Savitsky, P. A. and Finkel, T.** (2002). Redox regulation of Cdc25C. *J. Biol. Chem.* **277**, 20535-20540.
- Solmaz, S. R., Chauhan, R., Blobel, G. and Melčák, I.** (2011). Molecular architecture of the transport channel of the nuclear pore complex. *Cell* **147**, 590-602.
- Spickett, C. M., Pitt, A. R., Morrice, N. and Kolch, W.** (2006). Proteomic analysis of phosphorylation, oxidation and nitrosylation in signal transduction. *Biochim. Biophys. Acta* **1764**, 1823-1841.
- Stochaj, U., Rassadi, R. and Chiu, J.** (2000). Stress-mediated inhibition of the classical nuclear protein import pathway and nuclear accumulation of the small GTPase Gsp1p. *FASEB J.* **14**, 2130-2132.
- Stoffler, D., Fahrenkrog, B. and Aebi, U.** (1999). The nuclear pore complex: from molecular architecture to functional dynamics. *Curr. Opin. Cell Biol.* **11**, 391-401.
- Strawn, L. A., Shen, T., Shulga, N., Goldfarb, D. S. and Wentz, S. R.** (2004). Minimal nuclear pore complexes define FG repeat domains essential for transport. *Nat. Cell Biol.* **6**, 197-206.
- Terry, L. J. and Wentz, S. R.** (2007). Nuclear mRNA export requires specific FG nucleoporins for translocation through the nuclear pore complex. *J. Cell Biol.* **178**, 1121-1132.
- Weis, K.** (2003). Regulating access to the genome: nucleocytoplasmic transport throughout the cell cycle. *Cell* **112**, 441-451.
- Winterbourn, C. C.** (2008). Reconciling the chemistry and biology of reactive oxygen species. *Nat. Chem. Biol.* **4**, 278-286.
- Winterbourn, C. C. and Hampton, M. B.** (2008). Thiol chemistry and specificity in redox signaling. *Free Radic. Biol. Med.* **45**, 549-561.
- Yasuda, Y., Miyamoto, Y., Saiwaki, T. and Yoneda, Y.** (2006). Mechanism of the stress-induced collapse of the Ran distribution. *Exp. Cell Res.* **312**, 512-520.
- Yoshimura, S. H., Takahashi, H., Otsuka, S. and Takeyasu, K.** (2006). Development of glutathione-coupled cantilever for the single-molecule force measurement by scanning force microscopy. *FEBS Lett.* **580**, 3961-3965.